Coherent optical transients

A new branch of optical spectroscopy that deals with the optical analogs of spin transients such as NMR is providing unique ways to explore dynamic interactions in optically excited atoms, molecules and solids.

Richard G. Brewer

The dynamics of nuclear spins in atomic and molecular environments have been examined in exquisite detail over the past 27 years by the methods of pulsed nuclear magnetic resonance.1 The early discovery of the spin echo by Erwin Hahn2 and the transient nutation effect by Henry Torrey3 initiated the field by introducing coherent transient phenomena to radiofrequency spectroscopy. An entire class of coherent spin transients could be observed by a simple variation of the rf pulse sequence, and from the decay characteristics the various spin-dephasing mechanisms could be examined separately. In short, these methods allowed decomposition of the spin-transition linewidth into its broadening components, and also offered new and versatile ways for performing high-resolution rf spectroscopy.

Optical coherence is also a mature subject. Well known examples predating the laser are Young's two-slit interference effect, which demonstrates spatial coherence; the Michelson interferometer, which demonstrates temporal interference, and the Brown-Twiss experiment, which demonstrates an intensity-correlation effect. With laser light, however, a new class of optical coherence phenomena is now at hand, consisting of effects that are the optical analogs of spin transients. In this article I review this new branch of optical spectroscopy, which is providing unique ways for exploring dynamic interactions in optically excited atoms, molecules and solids.

The possibility of bringing the methods of pulsed NMR to the optical region was not immediately obvious. Because coherent radiation is required, optical studies were excluded prior to the laser, that is, before 1960. Furthermore, it was

not clear whether optical electric-dipole transitions behaved in the same way as the rf magnetic-dipole transitions of spin systems. This situation was clarified in a wellknown paper 4 of Robert Dicke, who showed that the two are equivalent. In either case, a collection of two-level quantum systems can be prepared coherently in superposition states, and these constitute a phased array of dipoles (electric or magnetic), which can emit coherent radiation as prescribed by Maxwell's equations.

The photo on the cover of this issue of PHYSICS TODAY shows one example of a coherent transient in the optical region; it is observed by a laser frequency-switching technique described below.

Maxwell-Bloch equations

The equivalence of magnetic- and electric-dipole transients was further demonstrated by Richard Feynman, Frank Vernon and Robert Hellwarth,⁵ who transformed the Schrödinger equation into the three-dimensional vector equation

$$\frac{d\beta}{dt} = \omega \times \beta \tag{1}$$

This has the form of the classical torque equation of motion for a spin precessing in a magnetic field and was used originally by Felix Bloch⁶ to describe NMR. Equation 1 is commonly referred to as the Bloch equation. It is a geometric representation of a two-level quantum system interacting resonantly with a radiation field, acting either through an electric- or a magnetic-dipole interaction. The precessional motion of the Bloch vector $\boldsymbol{\beta}$ about an effective field $\boldsymbol{\omega}$ (in frequency units) therefore applies to either situation, where we understand that the coordinate system in equation 1 rotates with

the angular frequency of the radiation field about the z axis.

For the spin- $\frac{1}{2}$ case, the Bloch vector β is a magnetic dipole moment with three projections in real space, and the effective field ω is the vector sum of a static magnetic field (along the z axis) and an rf magnetic field (along the x axis) in the rotating frame, all multiplied by the gyromagnetic ratio.

For a two-level quantum system interacting with an optical wave, the Bloch vector

$$\beta = \mathbf{i}u + \mathbf{j}v + \mathbf{k}w \tag{2}$$

does not lie in physical space, but rather in a mathematical space with components

$$u = \tilde{\rho}_{12} + \tilde{\rho}_{21}$$

 $v = i(\tilde{\rho}_{21} - \tilde{\rho}_{12})$ (3)
 $w = \rho_{22} - \rho_{11}$

where ρ is the density matrix and the rapidly oscillating factor is removed with the substitution $\rho_{12} = \tilde{\rho}_{12} \exp[i(\Omega t - kz)]$. This assumes an electric-dipole interaction $V = -\mu \cdot \mathbf{E}$ for an optical field $E = E_0 \cos(\Omega t - kz)$, which resonantly excites a transition $1 \to 2$ having a dipole matrix element μ_{12} and a transition frequency ω_{21} . Here, u and v represent the in-phase and out-of-phase components of the optically induced dipole

$$p = \text{Tr}(\mu \rho) \tag{4}$$

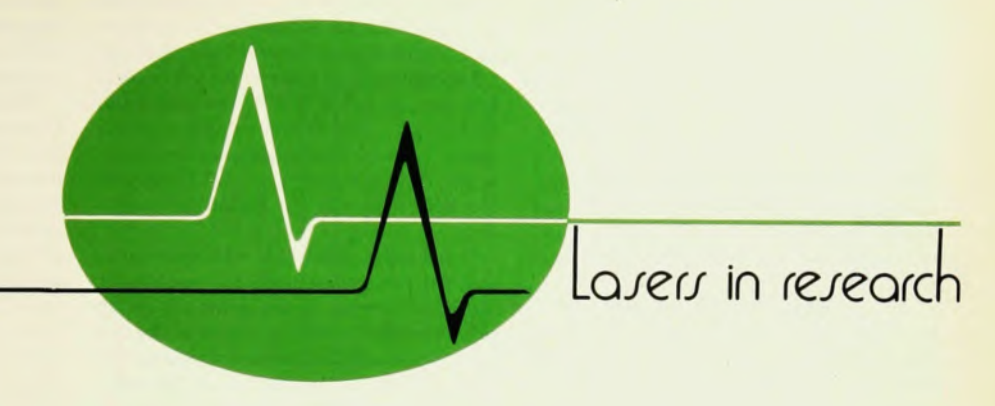
while the population difference of the transition levels is given by Nw, N being the atomic number density.

The effective field now takes the form

$$\omega = -i\chi + k\Delta \tag{5}$$

where χ is the Rabi flopping frequency $\mu_{12}E_0/h$. For the case of a moving atom with a velocity component v_z along the

Richard G. Brewer is an IBM Fellow at the IBM Research Laboratory in San Jose, California.



laser beam, the resonant tuning parameter, Δ , equals $\Omega + kv_z + \omega_{21}$ and the Doppler shift is kv_z .

The optically prepared dipoles given by equation 4 generate a coherent signal field

$$E_s(z,t) = \tilde{E}_s(z,t)e^{i(\Omega t - kz)}$$

which obeys Maxwell's wave equation in the slowly-varying-envelope approximation

$$\frac{\partial E_s}{\partial z} = -2\pi i k N \langle \tilde{p} \rangle \tag{7}$$

when the sample is optically thin, the dipole amplitude being $\tilde{p} = \mu_{12}\tilde{\rho}_{12}$. Because atomic and molecular environments are always inhomogeneous, the dipoles radiate with a distribution of frequencies and exhibit temporal interference. The angular bracket in equation 7 therefore sums over the *inhomogeneous* line broadening, which is due to Doppler broadening for a gas and to crystalline strain broadening for a solid.

Decay phenomena

With the inclusion of damping terms due to homogeneous line broadening, the coupled Maxwell-Bloch equations are sufficiently general to describe many spin and optical coherent transient phenomena. Decay due to atomic collisions, spontaneous radiative emission or other causes can depopulate the lower and upper transition levels, labelled 1 and 2 respectively, with phenomenological decay rates γ_1 and γ_2 .

In the density-matrix formulation of the Schrödinger equation,⁷ these rates correspond to decay of the diagonal elements ρ_{11} and ρ_{22} . As a consequence, the dipole and the off-diagonal element ρ_{12} dephase at the rate

$$\gamma = \frac{1}{2}(\gamma_1 + \gamma_2) \tag{8}$$

There also exist processes that disrupt the phase of the dipole without depopulating either level so that equation 8 becomes

$$\gamma = \frac{1}{2}(\gamma_1 + \gamma_2) + \gamma_{\phi} \tag{9}$$

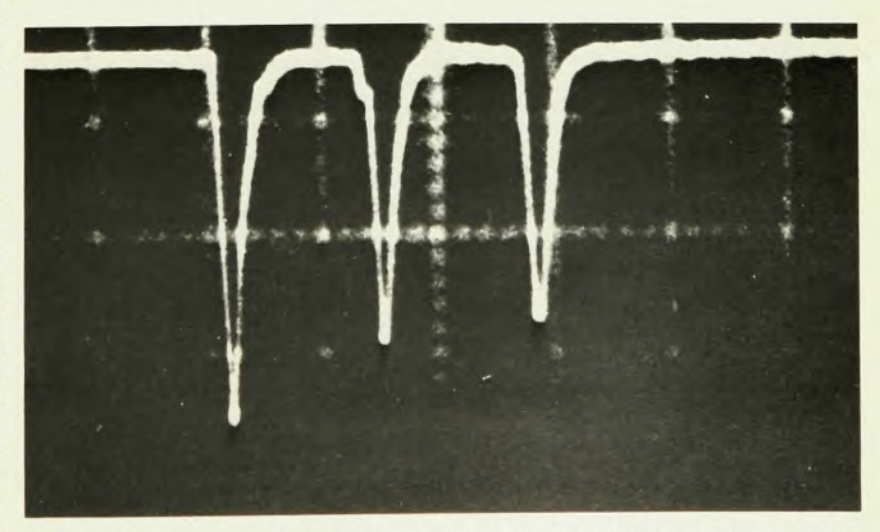
where γ_{ϕ} expresses the rate of phase interruptions.

When the radiative frequency changes with time because of spectral diffusion within the inhomogeneous line shape, the equations of motion must also be modified to allow for a decay that is no longer a simple exponential (see equation 11, below). In the language of NMR, the dipole terms u and v decay at the rate $1/T_2$ and the population term w decays at the rate $1/T_1$. In the above terms $\gamma = 1/T_2$, but T_1 is defined only when w is characterized by the single decay rate

 $1/T_1$, for example, when $\gamma_2 = \gamma_1$ or $\gamma_1 = 0$. The description in terms of T_1 and T_2 appears to be valid for transitions of molecular vibrational states in the infrared, as in NMR, but in the visible and ultraviolet regions the spontaneous emission rate can be large so that γ_1 and γ_2 are required, γ_2 as well as equations γ_2 and γ_3 .

Echoes, free induction decay, nutation

The spin-echo concept, extended to the optical region in 1964 by Norman Kurnit, Isaac Abella and Sven Hartmann, was the first example of this class of optical coherence effects. The group irradiated a ruby crystal with two short pulses of coherent light from a ruby laser and observed three equally spaced pulses in transmission, as shown in figure 1. The third pulse was a delayed spontaneous



A photon echo from a ruby sample at 4.2 K appears as a delayed third pulse after two successive ruby-laser pulses excite the crystal coherently. Time increases to the right at 100 nanosec/division. The photon echo was the first of a useful new class of optical coherence effects. Photo from N. A. Kurnit, I. D. Abella and S. R. Hartmann, reference 9.

burst of coherent light, which they called a photon echo by analogy with the spin echo.

These studies revealed that the electron spin of the optically excited chromium ion of ruby dephased due to the presence of the surrounding aluminum nuclei through the mutual flipping of the electronic and nuclear spins. The photon-echo method has been applied also in other ways and to other systems, for example, by Hartmann and co-workers to photon-echo nuclear double resonance in ruby and most recently to low-temperature organic solids. ¹⁰

An example of the photon-echo effect in a molecular gas¹¹ is shown in figure 2. The photon echo is an interference effect involving a coherent set of oscillating dipoles that dephase in the first pulse interval because of a spread in their frequencies (destructive interference) and rephase in the second pulse interval (constructive interference). The Bloch vector model shows this symmetric time behavior as a sequence of four precessional motions in figure 2 where the solutions of equation 1 are obtained by inspection.

Nutation For an initial laser pulse sufficiently long and intense, an atom will be driven first to the upper state (stimulated absorption) and then back to the lower state (stimulated emission), the cycle repeating thereafter until the end of the pulse. Since the laser beam is alternately absorbed and emitted by the sample, the intensity of the transmitted beam will display an oscillation as shown¹¹ in figure 3. This is the optical analog of the spinnutation transient; it was first seen by G. B. Hocker and Chung Tang, ¹² using a pulsed CO₂ laser, in an infrared transition of SF₆.

In terms of equation 1, the Bloch vector

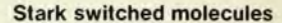
 β points in the -z direction for an atom initially in the lower state. With the application of a pulse, β precesses about the effective field $\omega = -i\chi + k\Delta$, causing the level-population difference (the projection of β on the z axis) and the dipole (the projection of β on the x-y plane) to oscillate at $\omega = (\chi^2 + \Delta^2)^{1/2}$, the precession frequency. For atoms exactly on resonance ($\Delta = 0$), the precession frequency is the Rabi frequency χ , and the higher the light intensity the faster the oscillation.

If the pulse width t_1 is now reduced so that the precession angle χt_1 equals $\pi/2$, the Bloch vector of the resonant group will be totally in the x-y plane at the end of the pulse and the induced dipole will be a maximum, as in part a of figure 2. From equation 4, the off-diagonal element ρ_{12} will be a maximum also, corresponding to an equal admixture of the upper- and lower-state wave functions.

Free induction decay Immediately after the pulse, the dipoles are in phase and, according to equations 6 and 7, emit an intense coherent beam of light. This emission, shown in figure 4, was demonstrated initially by Richard Shoemaker and me^{13} ; it is the optical analog of the free induction decay first seen by Hahn in NMR. Notice that because the fields of the N dipoles add in phase, the emission intensity will vary as N^2 and so will far exceed spontaneous emission, which varies as N. Because of momentum (or k) conservation, coherent emission can only occur in the forward direction.

In short, the emission due to free induction decay resembles the laser light that produced it, but with one difference: Because of inhomogeneous line broadening the dipoles radiate with a distribution of frequencies and thus interfere as time evolves, causing the emission to decay. The dephasing behavior of these frequency "packets" is seen in figure 2b, which shows the Bloch vector processing about $\omega = \mathbf{k}\Delta$ (since $\chi = 0$) for different frequencies Δ . We will now see that the echo is a free induction decay that has rephased.

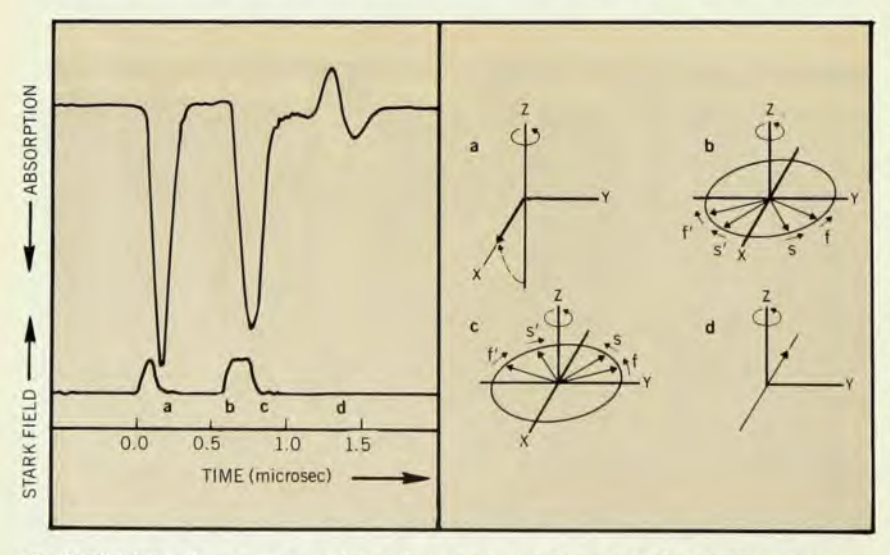
Photon echo The second laser pulse tips the Bloch vector so that the sign of the dipole phase is reversed. This is shown in figure 2c for the resonance case, where the pulse duration t_2 gives a precession angle $\chi t_2 = \pi$. Other tipping angles and A's give echoes with smaller amplitudes. Following the second pulse. each Bloch vector in figure 2c precesses about the effective field $\omega = \mathbf{k}\Delta$ in the same sense as during the first pulse interval, but because the slow packets (labelled "s" in the figure) lead the fast ones. "f," it is clear that all packets will come into phase precisely at time 27, where 7 is the pulse delay time. At this point the sample has a macroscopic dipole moment and will emit a burst of coherent lightthe photon echo. By this dephasingrephasing mechanism, the echo amplitude is unaffected by the large inhomogeneous linewidth, whereas the irreversible dephasing effects of homogeneous broadening remain.



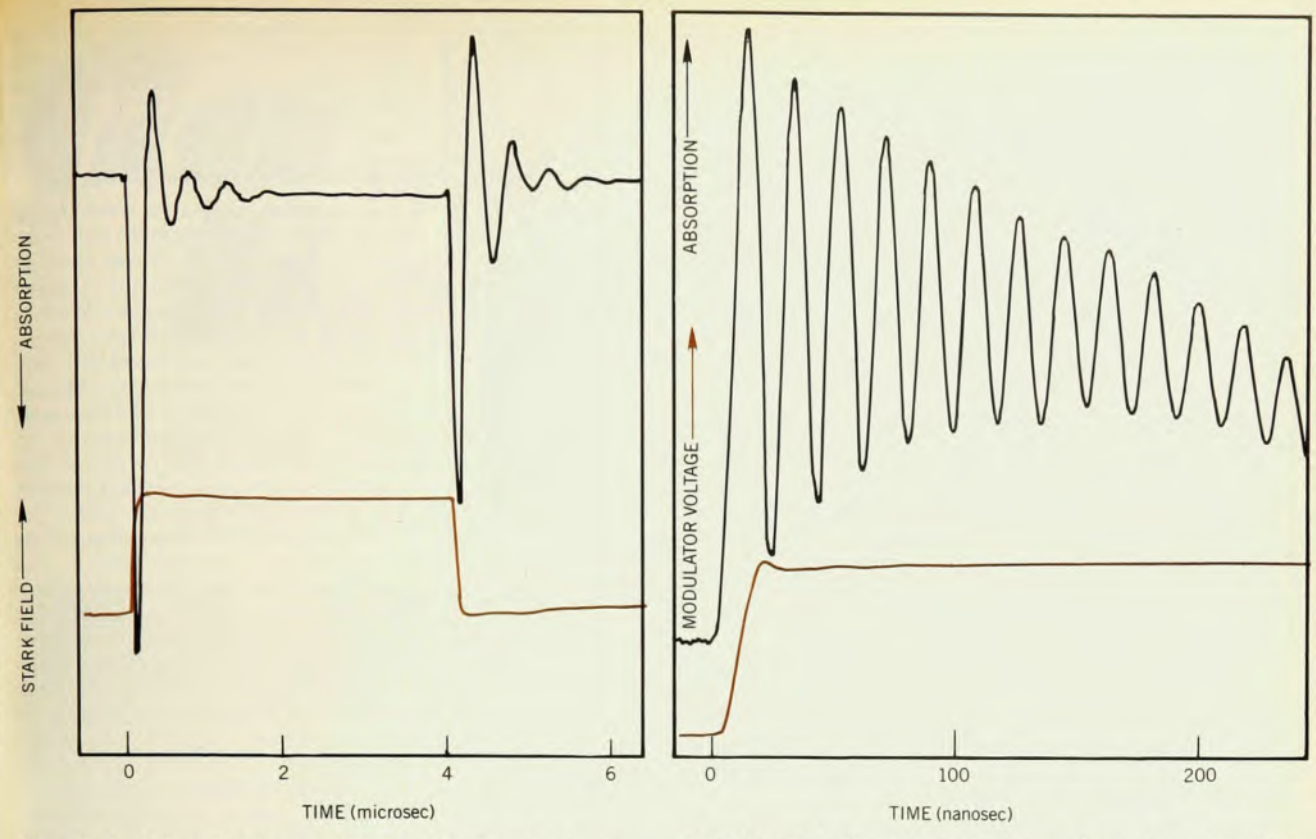
Optical studies have progressed rather slowly compared to the field of spin transients, because pulsed lasers are more difficult to control than rf pulse generators. A new method for observing coherent optical transients, particularly in the infrared, was introduced¹¹ by Shoemaker and me in 1971, and possesses several distinct advantages. In this case, the exciting laser radiation is cw and the molecular level splitting is pulsed. The apparatus is diagrammed in figure 5.

The underlying idea rests on the fact that molecules at a pressure of a few millitorr can exhibit exceedingly sharp optical resonances. Laser light, which is essentially monochromatic, will be strongly absorbed only when its frequency closely matches, to one part in 108-109, the molecular resonance frequency. If by some method the molecular transition frequency is shifted suddenly outside its homogeneous linewidth, the absorption can be switched on or off nonadiabatically. The switching mechanism used is the Stark effect, in which the application of a pulsed dc electric field allows molecules to be tuned to or away from the laser frequency. Instead of using pulsed laser light, which is difficult to control, the molecule's energy-level spacing is pulsed while the laser's frequency and intensity remain fixed in time.

The transients illustrated in figures 2 and 3 have been obtained in this way for a particular C¹³H₃F vibration-rotation transition in the 10-micron infrared region, which will be referred to throughout this article. The beam from a stable cw



The third pulse in the upper trace at the left is an infrared photon echo for a vibration–rotation transition in C¹³H₃F. The 60 V-cm Stark pulses shown in the lower trace switched the gas sample into resonance twice with a cw carbon-dioxide laser at 9.7 microns. The four diagrams at the right indicate four stages in the precessional motion of the Bloch vector, corresponding to the times marked a, b, c and d on the pulse sequence. From reference 11.



The optical nutation effect in methyl fluoride, C¹³H₃F, irradiated by a carbon-dioxide laser at 9.7 microns. The apparatus for this experiment as well as that of figure 2 is shown schematically in figure 5. The Rabi oscillations appear here because the 35-volt/cm Stark pulse (colored line) is longer than those in figure 2. From R. G. Brewer and R. L. Shoemaker, reference 11.

Optical free induction decay in I_2 vapor produces a heterodyne beat signal with frequency-shifted laser light. The sample is prepared with 5896-Å light from a cw dye laser; it radiates coherently when the frequency is abruptly switched 54 MHz by a 100-volt pulse. The slowly varying background is a nutation signal from a second velocity group. Figure 9 shows the experimental arrangement. (Ref. 18). Figure 4

CO₂ laser passes through the gas sample, which is contained in a Stark cell, before striking a photodetector that monitors the absorption or emission transients.

Imagine in figure 6 that, prior to a Stark pulse, a laser with frequency Ω selects from a molecule's Doppler line shape a particular velocity group vz, which it coherently prepares under steady-state conditions. When a Stark pulse appears, this group is switched out of resonance and freely radiates an intense, coherent beam of light at frequency Ω' in the forward direction-the free-induction-decay transient. At the same time, a second velocity group v, will be switched into resonance and will alternately absorb and emit laser radiation—the nutation effect. If two Stark pulses are applied, the group v₂ emits a third pulse—the photon

The important advantages inherent in the Stark switching technique now become evident:

The transient observed is the desired coherent transient itself, and the difficulty of separating a small transient signal from a time-coincident laser pulse of large amplitude is avoided.

Heterodyne detection occurs because the emission transient is displaced in frequency from the laser light by the Stark shift and together with the laser beam strikes a photodetector. This increases the free-induction-decay and echo signals by about three orders of magnitude and facilitates measuring their decay.

▶ The entire class of coherent optical transient effects can be monitored, because the electronic pulse sequence and pulse shape can be tailored conveniently to the particular experiment of interest. To date, some ten different coherent optical transient effects have been observed in this way.¹⁴

Molecular collisions

The Stark switching method is well suited to the study of molecular collision phenomena. 15 Elastic and inelastic scattering can be examined easily with two-pulse echoes and without the complication of Doppler broadening. This work complements the more elaborate molecular-beam technique and contrasts with traditional steady-state linewidth measurements, in which the broadening mechanisms are rarely disentangled. The two-pulse sequence of figure 2 provides two independent measurements as the pulse delay time is advanced:

The echo amplitude decreases because collisions dephase the coherently prepared dipoles.

▶ The second or delayed nutation signal

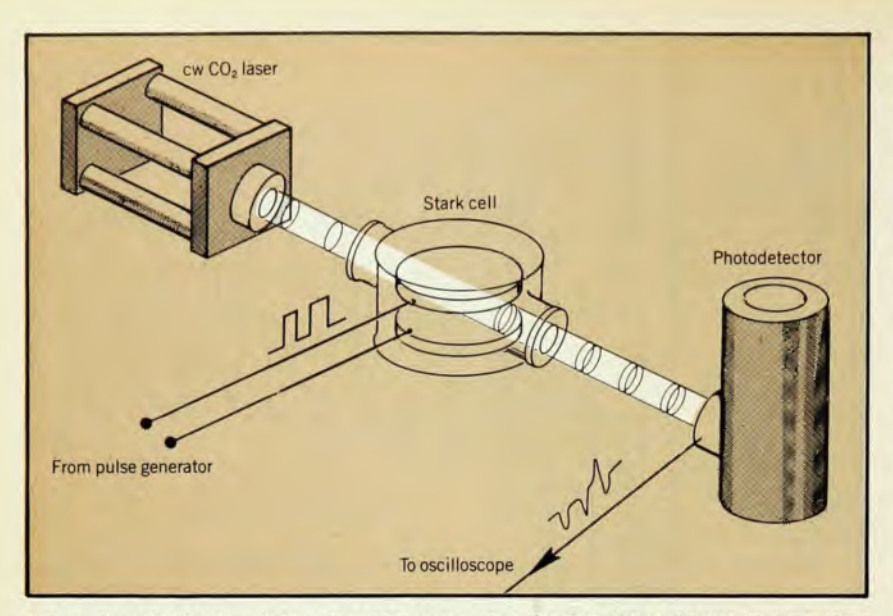
grows, due to collisions that partially restore the equilibrium population from the imbalance created by the first pulse.

The delayed nutation and echo amplitudes for $C^{13}H_3F$ are shown in figure 7 as a function of pulse delay time. The nutation signal (upper curve) displays the decay time (T_1) for inelastic collisions, the cross section being about 500 Å². Elastic collisions, on the other hand, alter the molecular velocity, causing the echo signal to deviate from the upper curve. Because a collision-induced velocity change Δv_z translates as a Doppler shift $k \Delta v_z$ and a corresponding phase shift $k \Delta v_z$ in time t, it is clear that even if Δv_z is small the dipoles will eventually get out of phase.

Writing the echo electric field in the form

$$E \propto (\exp(ik\Delta v_z t))$$

where () denotes a collision average, we can use a simple Brownian-motion argument 15 to derive the echo time dependence due to elastic collisions. Let Δu be $\sqrt{2}$ times the rms change in velocity per collision and τ the pulse delay time. When $k \Delta u \tau \gg 1$, any collision produces destructive phase interference so that the only contribution to the field average E that survives will be the one where no collision occurs up to the time of echo formation $t=2\tau$. Since the associated



Schematic of the Stark switching apparatus that is used for observing optical transients such as those illustrated in figures 2 and 3. From reference 11.

probability is $e^{-\Gamma t}$, where Γ is the rate of elastic collisions, one finds for long times

$$E(t = 2\tau) \propto \exp(-\Gamma t)$$

when $k \Delta u \tau \gg 1$ (10)

If, on the other hand, $k\Delta u\tau$ is much less than 1, each collision produces a small phase change such that $E \propto 1 - \frac{1}{2}k^2((\Delta v)^2)\tau^2$, where $(\Delta v) = 0$. With the collision average $((\Delta v)^2) = \Gamma t \Delta u^2/2$, we get for short times

$$E(t = 2\tau) \propto \exp[-\Gamma t^3 (k\Delta u)^2/16]$$
when $k\Delta u\tau \ll 1$ (11)

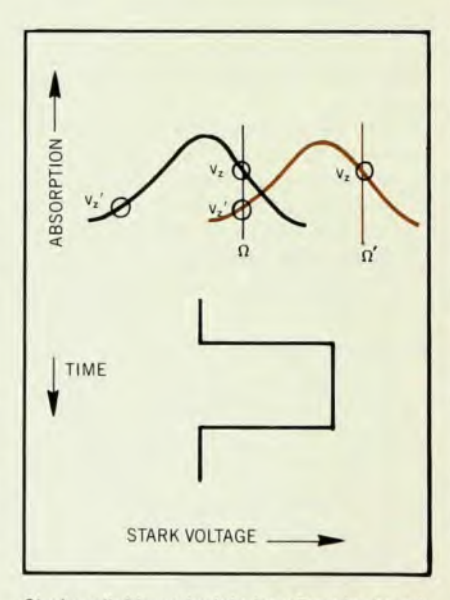
It agrees essentially with a more rigorous theory based on the Boltzman transport equation.¹⁵

These calculations also agree with the experiments of figure 7 and constitute primary evidence that elastic molecular collisions involving small changes in velocity play a crucial role in infrared photon echoes. The cubic decay law (equation 11) is reminiscent of the dephasing that occurs in spin echoes when spin diffusion in liquids takes place in a magnetic-field gradient.2 In these optical experiments diffusion occurs in velocity space due to low-angle elastic scattering, for which the characteristic velocity jump per collision in $C^{13}H_3F$ is only $\Delta u = 85$ cm/sec and the corresponding total cross section is about 430 Å2.

Carr-Purcell echoes A variation on this theme is to replace the two-pulse echo by an n-pulse echo sequence, which is easily done by applying n+1 Stark pulses. ¹⁵ If the pulse interval τ is short enough, velocity or spectral diffusion can be made negligible, and the decay time of the echo envelope function is the residual dipole-dephasing time, simply T_2 . This is demonstrated in figure 7, where we see,

from the coincidence of the Carr–Purcell and nutation-decay curves, that $T_2 = T_1$. The n-pulse photon echo is an optical version of the NMR method of Herman Carr and Edward Purcell. ¹⁶

The basic concept can be explained by noticing that for an n-pulse echo train with short pulse intervals τ , the amplitude of the last echo at time $t = 2n\tau$ is given by the nth power of the field E in equation 11; that is, $[\exp(-8K\tau^3)]^n = \exp(-Kt^3/2)$



Stark switching principle for a Doppler-broadened transition. The laser, of fixed frequency Ω , initially excites molecules of velocity v_z . A Stark pulse that abruptly shifts the molecular transition frequency from the black to the colored curve causes the velocity group v_z to emit the free induction decay signal at frequency Ω' , while the group with velocity v_z' exhibits nutation. With two pulses, the group v_z' emits an echo.

 n^2). In comparison to that given by equation 11 for a two-pulse echo over the same time interval t, it is evident that the Carr-Purcell decay time is n^2 times longer.

Fourier-transform spectroscopy

The method of Fourier transforming transient phenomena from the time to the frequency domain has proven to be an extremely versatile technique in pulsed nuclear magnetic resonance. With it, ultrahigh-resolution NMR spectroscopy can be performed quickly and with high sensitivity in a set of densely spaced lines. Furthermore, because the NMR signals display coherent transient behavior, dynamic information about nuclear spin interactions can be derived in a selective manner for each transition as well.

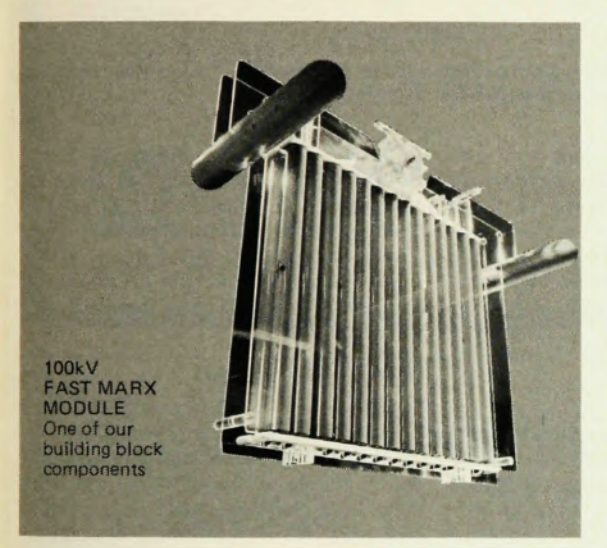
An application of this technique in the optical region¹⁷ is shown in figure 8. The spectrum is obtained from several C13H3F transitions that produce two-pulse photon echoes simultaneously. By advancing the pulse delay time, the echo decay for each transition can be monitored also. This yields a three-dimensional diagram of echo amplitude versus frequency and elapsed time. Measurements are performed with the Stark switching apparatus, which is now interfaced with a computer for rapid Fourier analysis. The four lines are actually heterodyne beat signals of the same Stark-split C13HaF vibration-rotation transition, the v3 mode $(J,K,M) = (4,3,M) \rightarrow (5,3,M)$ mentioned earlier, each beat frequency being due to two transitions with $M \rightarrow M$ and $-M \rightarrow$ -M. The lines are 170 kHz wide, are spaced at 0.83-MHz intervals and clearly display a Doppler-free behavior, as the Doppler width is 66 MHz. From echo and free-induction-decay measurements of this kind, elastic and inelastic scattering can be studied independently again, but since the lines are now resolved, the cross sections can be obtained as a function of quantum state and molecular velocity. This degree of flexibility offers stringent tests of existing scattering theories and is being used to study the force laws that dominate molecular collisions.

Laser frequency switching

Azriel Genack and I recently reported a general method for observing coherent transients in the visible-ultraviolet region¹⁸ (Search and Discovery, PHYSICS TODAY, October 1976, page 17). The technique, diagrammed in figure 9, requires switching the laser frequency into or out of resonance with the sample; it is equivalent to the Stark switching method. However, when the source is a stable tunable cw dye laser, this approach is more universal in its application, particularly because the need for Stark tunable molecules is removed. Laser frequency switching is exceedingly simple and can be achieved merely by driving an elec-

GO THE BOMPONIENTS

HIGH VOLTAGE COMPONENTS FOR YOUR LASER RESEARCH









Please accept our invitation to visit our booth (420) at CLEA 77, June 1 - 3

in Germany POTSCHKE & CO. KG. D-6000 BERGEN-ENKHEIM 1 POSTFACH 225 FED. REP. OF GERMANY Telex: 04-1859 41 in France
EQUIPMENTS
SCIENTIFIQUES S.A.
35 Chemin des Roses, 92150
SURESNES (France)
Telex: Scientif. 61 707 F

U.S.A. TWX (910) 366-7033

in Japan HAKUTO CO., LTD. C. P. O. Box 25 Tokyo 100-91 Japan Telex: J22912A J22912B



2700 Merced Street / San Leandro, Ca 94577 / Tel (415) 357-4610

Circle No. 32 on Reader Service Card

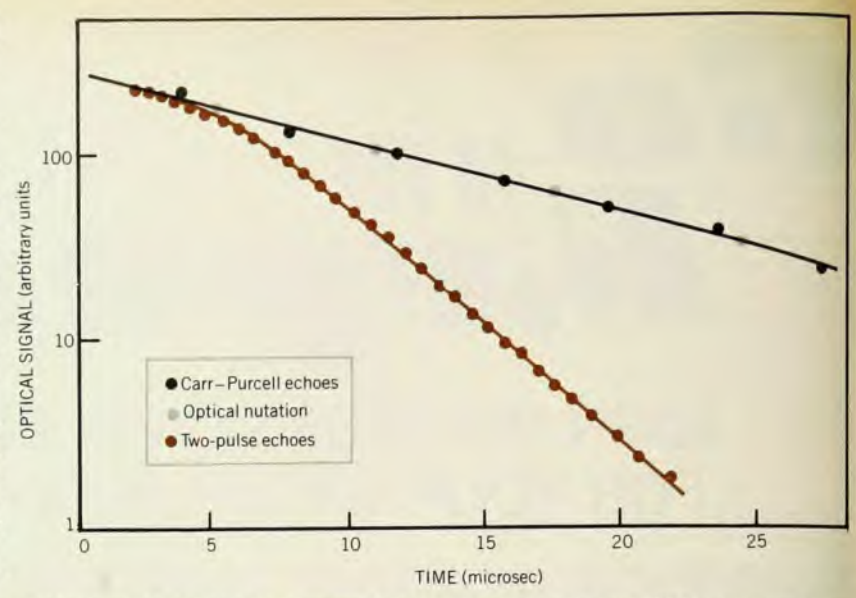
tro-optic crystal (ammonium dihydrogen phosphate), which is inside the dye laser cavity, with the desired sequence of lowvoltage pulses.

The time-dependent variations in the refractive index of the electro-optic element produce corresponding changes in the optical cavity length, and hence in the laser frequency. Dynamically the effect is equivalent to the Doppler shift the laser beam would experience on being reflected by a moving end mirror of the cavity. The frequency shift therefore occurs almost instantaneously. The switching time is limited by the transit time of light through the ADP crystal, about 50 picosec, and not by the rise time of the voltage pulse or by the laser-cavity ringing time, about 25 nanosec. In addition, the frequency-shifted light is stored in the optical cavity and amplified in the same way that the unshifted light was.

Clearly, a resonant sample exposed to frequency-switched laser light will experience coherent transient behavior. Because the experiment is controlled electronically, all of the advantages inherent in the Stark switching technique are preserved here as well. Moreover, with the large tuning range of the dye laser, measurements are equally feasible in atoms, molecules and solids.

In initial studies in molecular iodine vapor, effects such as free-inductiondecay (figure 4), nutation and echoes are easily monitored in the visible. Because the signal-to-noise ratio is high, about 103, it has been possible to test the theory of these transient phenomena quantitatively and in complete detail. From two-pulse nutation and echo studies of I2 it is found that elastic collisions are not of the velocity-changing type, as in the infrared, but rather are due to collision-induced frequency shifts. In this case, the echo decays exponentially with a decay rate given by equation 9, in contrast to equation 11. Apparently, excited electronic states are more sensitive to perturberinduced frequency shifts than vibrationally excited states are. This appears to be the first optical-coherence measurement of phase-interrupting collisions.

In a solid, laser frequency switching has been used at IBM to measure the dephasing time of coherently prepared impurity ions of praseodymium in a lowtemperature LaF3 host crystal.19 Freeinduction decay is monitored and possesses certain advantages over the echo technique. As can be seen in figure 4, the entire decay is obtained in a single burst following a step-function switching pulse. Because of the sensitivity offered by heterodyne detection, weak transitions can be studied at laser powers as low as 50 microwatts. At laser power levels, where $\chi^2 \ll 1/(T_1 T_2)$, the free-induction-decay time is simply $\frac{1}{2}T_2$ where the $\frac{1}{2}$ factor arises because T2 determines the inhomogeneous bandwidth during steady-state preparation and adds an additional $1/T_2$



Decay curves for three coherent infrared transient effects, observed in C¹³H₃F by Stark switching The Carr–Purcell and nutation curves coincide. From reference 15.

decay rate. The rather long Pr^{3+} dephasing time of 0.38 microsec corresponds to an extremely narrow linewidth of 830 kHz (resolution: 6×10^8) and is unaffected by phonons below 4 K, power broadening, Pr^{3+} – Pr^{3+} interactions or the large inhomogeneous width of 4 GHz arising from crystal strains. On the other hand, it far exceeds the 640-Hz limit due to spontaneous radiative decay of the upper level.

Magnetic hyperfine interactions constitute a possible dephasing mechanism currently under study by several groups including Hartmann (Columbia University), Lynden Erickson (NRC, Ottawa) and Raymond Orbach (UCLA). Thus these measurements begin to invade a time scale ranging from microseconds to milliseconds and will impose significant demands on laser frequency stability.

At the other extreme, the fastest dephasing time measured by laser frequency switching is about 8 nanosec, as seen in the free induction decay of the sodium D lines. It will be challenging to see whether this method can be extended in the future to even shorter times, perhaps to the 50-picosec range.

Picosecond pulse generation

A related development, intense optical pulses of 30 picosec duration generated by free induction decay in a high-density gas, has attracted interest in laser fusion. ²⁰ In the preparative step, a CO₂ laser pulse 200 nanosec long and 1 MW in power passes through a pair of lenses before resonantly exciting a CO₂ gas sample at a pressure of about 250 Torr. At a certain time during the pulse the excitation ends abruptly, due to dielectric breakdown of the gas in the focal region between the lenses; at this point free induction decay commences. Because nearly all of the laser light was

absorbed during preparation, the emission will be intense initially and thereafter will decay in the time $T_2/(\alpha L)$ when $\alpha L > 1$; here α is the absorption coefficient and L the sample length. Hence, in this high-density regime, the decay can be considerably faster than the dipole-dephasing time T_2 .

Two-photon transients

The one-photon processes considered up to this point are for the most part optical analogs of NMR transient phenomena. Coherent two-photon transients have been observed in the optical region also and provide additional information about dephasing processes.

Picosecond studies Foremost among the two-photon processes are the Raman transients, which were exploited in simple liquids by Wolfgang Kaiser and his coworkers,21 who used picosecond laser pulses, as from a mode-locked neodymium glass laser of wavelength 1.06 microns. (See also the accompanying article by Marc Levenson on steady-state aspects of Raman scattering in this issue of PHYSICS TODAY.) Vibrational decay times on a picosecond time scale have been obtained by first generating a coherent vibrational excitation and Stokes light through the stimulated Raman process. A weak delayed second pulse then probes the remaining vibrational excitation by generating phase-matched anti-Stokes radiation. The vibrational dephasing time is monitored through the dependence of the anti-Stokes intensity on pulse delay time. In liquid carbon tetrachloride, for example, the totally symmetric vibrational mode shows a dephasing time T_2 of 3.6 picosec. Moreover, the decay exhibits beats at a frequency of about 1011 Hz, due to the different isotopic species Cl35 and Cl37.

Now you can interface your Varian Computer with CAMAC

Nuclear Enterprises' 9030 CAMAC Controller makes it possible for you to interface your CAMAC system with your Varian computer. The 9030 uses a removable interface card designed specifically for the computer you're using to provide direct, crate-to-computer interface.

To use a different computer, just insert the appropriate interface card. Interface cards are available for PDP 8 and 11, Hewlett-Packard, Honeywell, and many other computers in addition to Varian.

The 9030 will handle dedicated-crate systems, as well as multicrate and multibranch systems of up to 56 crates.

Call or write:



Nuclear Enterprises, Inc. 931 Terminal Way San Carlos, California 94070 (415) 592-8663 Telex 348-371

Associate company, Nuclear Enterprises, Ltd., Edinburgh, Scotland

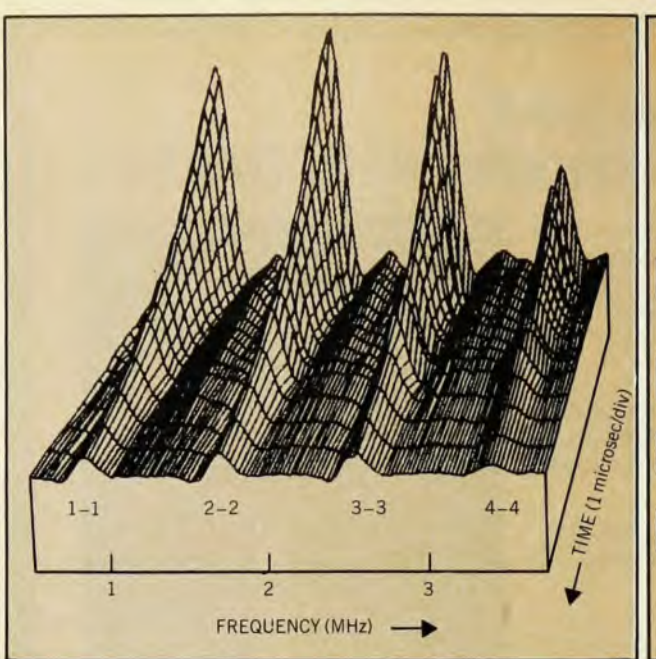


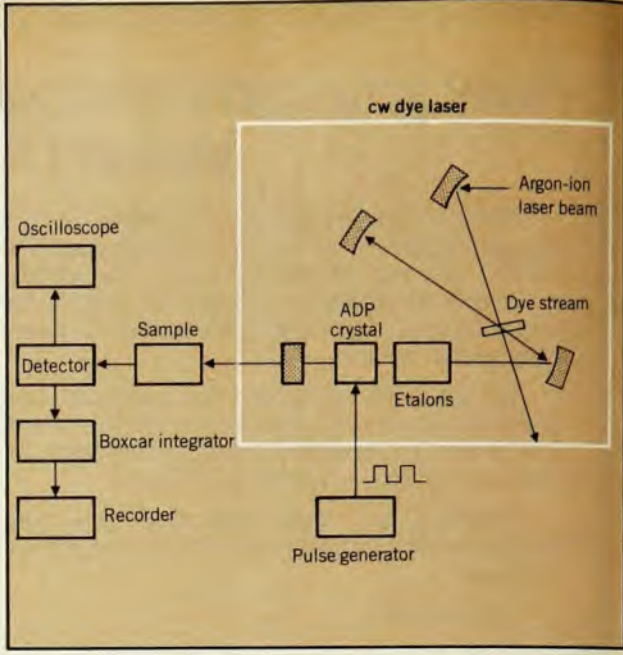
Circle No. 33 on Reader Service Card



©1977 MARKAD SERVICE CO./all rights reserved N-39

Willoughby, Ohio 44094





A Fourier-transform spectrum of C¹³H₃F, derived from Stark-switched two-pulse photon echoes, shows beats in this three-dimensional diagram of echo amplitude as a function of frequency and pulse-delay time. The vibration-rotation transitions 1–1, 2–2, . . . , exhibit decay with increasing pulse delay time. From reference 17.

Laser frequency switching apparatus for observing coherent optical transients. In the box is a commercial cw dye laser with an electro-optical crystal of ammonium dihydrogen phosphate. When the crystal is driven by low-voltage dc pulses its refractive index changes, abruptly changing the laser frequency. From reference 18.

Raman echoes Stimulated spin-flip Raman scattering has been used to induce coherent spin states22 of bound donors in n-type CdS at 1.6 K, in the same way that vibrational modes are prepared coherently in molecular liquids. This is accomplished by exciting the sample with a pulsed dye laser at 4905 Å with two modes having a frequency difference $\omega_L - \omega_R =$ 32 GHz, which is just resonant with a pair of Zeeman-split spin states. After pulse preparation the spins dephase, as in free induction decay, and if a second optical pulse is applied the spins will rephase, as in an echo experiment. The spin dephasing-rephasing behavior can be monitored optically by suitably delaying a weak probe laser pulse at 4880 Å to produce Stokes scattering. The probe Raman scattering is enhanced at the time the spins have rephased and is called the Raman echo. Echoes of this type, which were predicted by Hartmann, have been observed22 with delay times to 162 nanosec in dilute samples of CdS (of density 8 $\times 10^{15} \,\mathrm{cm}^{-3}$).

Coherent Raman beats A different manifestation²³ of a two-photon transient can be found in a molecular gas with the Stark switching technique when three molecular levels are prepared initially in superposition by means of continuous laser radiation. We imagine that two of the levels (1 and 2) are degenerate and connect optically with a third (3) during a resonant steady-state preparative phase. With the sudden application of a dc Stark field, the molecular level degeneracy is broken and the laser beam is no longer in resonance with the one-photon transi-

tions, $1 \leftrightarrow 3$ and $2 \leftrightarrow 3$. However, the laser beam can now scatter off the coherently prepared sample in a two-photon process $1 \leftrightarrow 2$; that is, coherent forward Raman scattering can occur in the presence of the same laser field during the nonresonant condition. The two beams—the laser beam with frequency Ω and the Raman light with frequency $\Omega \pm \omega_{21}$ —strike a photodetector, where they produce a coherent beat at frequency ω_{21} . This is just the level splitting between initial and final states in the two-photon process.

From energy conservation, we see that the first-order Doppler shift kv_z in the first half of the two-photon process $(1 \leftrightarrow 3)$ essentially cancels that of the second half $(3 \leftrightarrow 2)$, making the overall process $1 \leftrightarrow 2$ independent of Doppler shift. As a result, inhomogeneous dephasing and elastic collisions that change the molecular velocity do not alter the decay rate of the Raman beat signal. That the decay will be determined only by inelastic collisions, in contrast to the two-pulse echo results, is corroborated by theoretical arguments and experiments. 15,23

Two-photon nutation A two-photon transient can be induced also by the sudden application of two light pulses of frequency Ω_1 and Ω_2 , such that the transition $1 \rightarrow 2$ satisfies the resonance condition $\Omega_1 + \Omega_2 = \omega_{21}$. In this case the energy of the intermediate level 3 lies roughly half way between 1 and 2, and the two waves must be counterpropagating so that the Doppler shifts nearly cancel, as in the Raman beat effect. Exact pulse or steady-state density-matrix solutions²³

for the three-level problem show in fact that the Raman beat effect with a single beam and two-photon absorption of oppositely directed laser beams are basically the same phenomenon, the difference being one of level configuration. The pulse solutions also reduce in an appropriate limit to a simple Bloch vector model,24 resembling equation 1, as it involves only the initial and final states in the overall transition $1 \rightarrow 2$. The intermediate level does not enter explicitly when the pulses are applied slowly (adiabatically) with respect to the frequency offset of the intermediate level, that is, when the intermediate transitions are nonresonant.

Michael Loy²⁵ has observed an infrared two-photon vibrational transient of this type in ammonia, which is induced by two counterpropagating CO₂ laser pulses. The transient oscillates because of the nutation effect, in quantitative agreement with the two-photon vector model. It is interesting that two-quantum transients in NMR are now also being explored.

Milliseconds to picoseconds

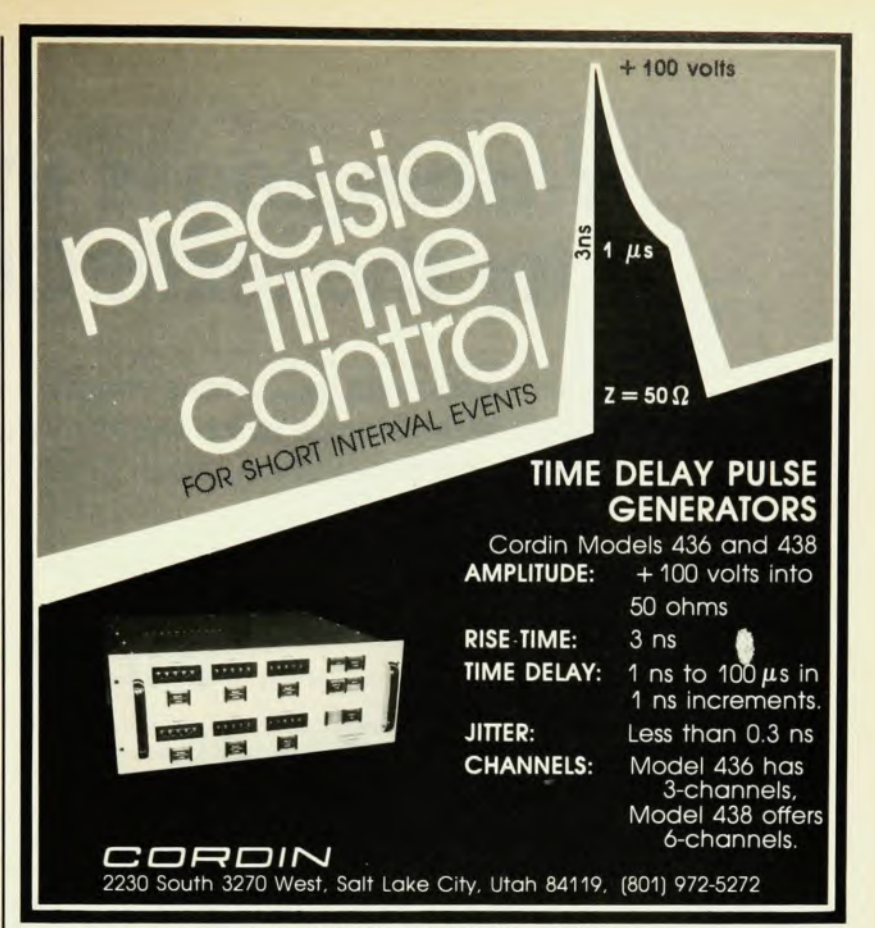
New ways for observing a class of coherent optical transient phenomena—measurements that resemble pulsed NMR transients—are now possible with the availability of laser radiation. Other novel effects²⁶ such as superradiance, quantum beats, adiabatic rapid passage and self-induced transparency, which were not discussed here, could have been included as well. Many of these coherence effects are just beginning to be useful in examining energy transfer and de-

phasing processes in optically excited atoms, molecules and solids, with time scales spanning the range from milliseconds to picoseconds.

The author gratefully acknowledges the thoughtful comments and criticisms of A. Z. Genack and A. Szöke. This work was supported in part by the US Office of Naval Research.

References

- A. Abragam, The Principles of Nuclear Magnetism, Oxford, London (1961).
- E. L. Hahn, Phys. Rev. 80, 580 (1950);
 PHYSICS TODAY, Nov. 1953, page 4.
- 3. H. C. Torrey, Phys. Rev. 76, 1059 (1949).
- 4. R. H. Dicke, Phys. Rev. 93, 99 (1954).
- R. P. Feynman, F. L. Vernon, R. W. Hellwarth, J. Appl. Phys. 28, 49 (1957).
- 6. F. Bloch, Phys. Rev. 70, 460 (1946).
- M. Sargent III, M. O. Scully, W. E. Lamb Jr, Laser Physics, Addison-Wesley, Reading, Mass. (1974), page 84.
- A. Schenzle, R. G. Brewer, Phys. Rev. A 14, 1756 (1976).
- N. A. Kurnit, I. D. Abella, S. R. Hartmann, Phys. Rev. Lett. 13, 567 (1964); Phys. Rev. 141, 391 (1966); S. R. Hartmann, Scientific American, April 1968, page 32.
- T. J. Aartsma, D. A. Wiersma, Phys. Rev. Lett. 36, 1360 (1976); A. H. Zewail, T. E. Orlowski, D. R. Dawson, Chem. Phys. Lett. 44, 379 (1976).
- R. G. Brewer, R. L. Shoemaker, Phys. Rev. Lett. 27, 631 (1971).
- G. B. Hocker, C. L. Tang, Phys. Rev. Lett. 21, 591 (1968).
- R. G. Brewer, R. L. Shoemaker, Phys. Rev. A 6, 2001 (1972).
- 14. R. G. Brewer, in Proceedings of the Les Houches Summer School Lectures, Volume I, Applications of Lasers to Atomic and Molecular Physics, Les Houches, France, 1975 (R. Balian, S. Haroche, S. Liberman, eds.), North-Holland (in press).
- P. R. Berman, J. M. Levy, R. G. Brewer, Phys. Rev. A 11, 1668 (1975).
- H. Y. Carr, E. M. Purcell, Phys. Rev. 94, 630 (1954).
- S. B. Grossman, A. Schenzle, R. G. Brewer, Phys. Rev. Lett. 38, 275, 1977.
- R. G. Brewer, A. Z. Genack, Phys. Rev. Lett. 36, 959 (1976).
- A. Z. Genack, R. M. Macfarlane, R. G. Brewer, Phys. Rev. Lett. 37, 1078 (1976).
- E. Yablonovitch, J. Goldhar, Appl. Phys. Lett. 25, 580 (1974); 30, 158 (1977).
- A. Laubereau, G. Wochner, W. Kaiser, Phys. Rev. A 13, 2212 (1976).
- P. Hu, S. Geschwind, T. M. Jedju, Phys. Rev. Lett. 37, 1357 (1976).
- R. L. Shoemaker, R. G. Brewer, Phys. Rev. Lett. 28, 1430 (1972); R. G. Brewer, E. L. Hahn, Phys. Rev. A 11, 1641 (1975).
- D. Grischkowsky, M. M. T. Loy, P. F. Liao, Phys. Rev. A 12, 2514 (1975).
- M. M. T. Loy, Phys. Rev. Lett. 36, 1454 (1976).
- L. Allen, J. H. Eberly, Optical Resonance and Two Level Atoms, Wiley, New York (1975).



Circle No. 35 on Reader Service Card



Circle No. 36 on Reader Service Card